Journal of Membrane Science 392–393 (2012) 66–75

Contents lists available at SciVerse ScienceDirect

Journal of Membrane Science

journal homepage: www.elsevier.com/locate/memsci

Quantitative measurement and visualization of biofilm O_2 consumption rates in membrane filtration systems

E.I. Prest[a,e,*], M. Staal[b], M. Kühl[b,c,d], M.C.M. van Loosdrecht[e], J.S. Vrouwenvelder[a,e,f]

[a] Wetsus, Centre of Excellence for Sustainable Water Technology, Agora 1, P.O. Box 1113, 8900 CC Leeuwarden, The Netherlands
[b] Marine Biological Section, Department of Biology, University of Copenhagen, Strandpromenaden 5, DK-3000 Helsingør, Denmark
[c] Plant Functional Biology and Climate Change Cluster, Department of Environmental Science, University of Technology Sydney, Australia
[d] Singapore Center for Environmental Life Sciences Engineering, Nanyang Technological University, Singapore
[e] Department of Biotechnology, Faculty of Applied Sciences, Delft University of Technology, Julianalaan 67, 2628 BC Delft, The Netherlands
[f] King Abdullah University of Science and Technology, Water Desalination and Reuse Center, Thuwal, Saudi Arabia

ARTICLE INFO

Article history:
Received 5 September 2011
Received in revised form
30 November 2011
Accepted 1 December 2011
Available online 19 December 2011

Keywords:
Optode
Non-destructive biofouling diagnosis
Biological activity measurement
Flow channels
Concentration polarization

ABSTRACT

There is a strong need for techniques enabling direct assessment of biological activity of biofouling in membrane filtration systems. Here we present a new quantitative and non-destructive method for mapping O_2 dynamics in biofilms during biofouling studies in membrane fouling simulators (MFS). Transparent planar O_2 optodes in combination with a luminescence lifetime imaging system were used to map the two-dimensional distribution of O_2 concentrations and consumption rates inside the MFS. The O_2 distribution was indicative for biofilm development. Biofilm activity was characterized by imaging of O_2 consumption rates, where low and high activity areas could be clearly distinguished. The spatial development of O_2 consumption rates, flow channels and stagnant areas could be determined. This can be used for studies on concentration polarization, i.e. salt accumulation at the membrane surface resulting in increased salt passage and reduced water flux. The new optode-based O_2 imaging technique applied to MFS allows non-destructive and spatially resolved quantitative biological activity measurements (BAM) for on-site biofouling diagnosis and laboratory studies. The following set of complementary tools is now available to study development and control of biofouling in membrane systems: (i) MFS, (ii) sensitive pressure drop measurement, (iii) magnetic resonance imaging, (iv) numerical modelling, and (v) biological activity measurement based on O_2 imaging methodology.

1. Introduction

High pressure membrane filtration processes such as nanofiltration or reverse osmosis can produce high quality drinking water. However, biofouling of the membrane can lead to operational problems such as a pressure drop increase over the feed spacer channel [1], and such biofilm formation is considered the major problem for membrane filtration processes [2–4].

Hitherto, biofouling diagnosis usually required macroscopic measurements such as pressure drop and subsequent membrane autopsy involving destructive opening and inspection of the membrane module to analyse the fouling material causing the pressure drop increase [2,5]. The pressure drop increase is indicative for fouling development in the feed spacer channel but is not conclusively linked to biofouling, as e.g. particulate material can also cause a pressure drop increase. Furthermore, pressure drop measurements do not provide spatial information on fouling development. Tools such as the membrane fouling simulator (MFS) were designed for early warning of biofouling and systematic laboratory studies on biofouling [6]. Other new tools such as magnetic resonance imaging (MRI) and numerical modelling have recently been used to get better insight in the spatial variation of biofouling processes in membrane systems. MRI can give spatially resolved data on fluid flow profiles and biomass [7,8], while a modelling approach based on biofilm growth, hydrodynamics and permeate production gives insights into the processes that lead to development of biofilms and flow channels within a feed spacer channel [9,10]. Use of these methods increases the understanding

Abbreviations: AOC, assimilable organic carbon; AOI, area of interest; ATP, Adenosine-Tri-Phosphate; BAM, biological activity measurement; BDOC, biodegradable dissolved organic carbon; BFR, biofilm formation rate; EPS, extracellular polymeric substances; LED, light emitting diode; MFS, membrane fouling simulator; MRI, magnetic resonance imaging; NMR, nuclear magnetic resonance; TDC, total direct cell count.

* Corresponding author. Present address: Department of Biotechnology, Faculty of Applied Sciences, Delft University of Technology, Julianalaan 67, 2628 BC Delft, The Netherlands. Tel.: +31 0 681327066; fax: +31 0 15 27 82355.
E-mail address: E.I.E.D.Prest@tudelft.nl (E.I. Prest).

0376-7388/$ – see front matter © 2011 Elsevier B.V. All rights reserved.
doi:10.1016/j.memsci.2011.12.003

Table 1
Scheme of tools to study and diagnose biofouling and for development and evaluation of biofouling control strategies.

Tool	Non destructive	Biological activity	Direct	Measurements	Information acquired	References
Membrane autopsy	No	Yes	No	Biomass parameters (e.g. ATP, TOC) Visual observations	Biofouling diagnosis	[5,28]
MFS	Yes	No	Yes	Pressure Drop Visual observations Autopsy	Early warning Biofouling development Biofouling diagnosis	[6,19,24,26]
Sensitive pressure drop	Yes	No	Yes	Differential pressure drop	Increase of friction caused by fouling	[18,19]
MRI	Yes	No	Yes	Structural imaging Velocity imaging Distributions of molecular displacement of passive tracers	Biomass amount and location Hydrodynamics	[7,29]
BAM[a]	Yes	Yes	Yes	Oxygen distribution Oxygen consumption	Biofouling diagnosis Biomass activity	This paper
Numerical model					Understanding of parameters and processes determining biofouling	[9,10,30]

[a] Combined with MFS.

of biofouling processes but non-destructive information on biofilm activity is still lacking (Table 1).

Molecular oxygen (O_2) is considered as a key parameter in biological systems [11], where O_2 concentrations vary significantly in space and time due to transport limitation, heterogeneity in biomass distribution and variations in O_2 consumption rates. Such heterogeneity in O_2 concentrations is indicative for structural heterogeneity within biofilms, while variations in O_2 consumption can be used as an indicator for biological activity distribution in biofilms. Two dimensional O_2 measurements can be used to visualize such heterogeneity and can be quantified with planar O_2 optodes. These optical sensors are based on luminescent O_2 sensitive dyes that can be fixed on supports, e.g. transparent carrier foils or glass windows. The development of planar optodes was a great improvement for studies linking biofilm structure and heterogeneity to the chemical dynamics [12–14]. Especially, the use of transparent planar optodes enables detailed mapping of O_2 distribution in combination with imaging structural information in biofilms [14–16]. Planar optodes have mainly been used for studies on heterogeneity of two dimensional O_2 distributions in sediments and biofilms [13,14] and only recently has this methodology been introduced in biofouling studies of membrane systems by Staal et al. [17], who briefly compared various O_2 imaging methods and their suitability for application in MFS.

In this study we present the first detailed planar O_2 optode study of biofilm formation in a MFS. The objective was to determine whether planar optodes would be a suitable tool to determine non-destructively the development and activity of biomass in a membrane fouling simulator. We monitored spatio-temporal changes in O_2 concentration and consumption rates and linked such measurements to other imaging techniques mapping biomass and flow distribution in the MFS.

2. Materials and methods

The set-up to study O_2 distribution and dynamics during the biofouling study consisted of three parts: (i) a membrane fouling simulator with equipment for water flow and substrate dosage (2.1), (ii) an imaging system to map the liquid flow distribution using the dye rhodamine WT (2.2) and (iii) a luminescence lifetime camera system for O_2 imaging (2.3).

2.1. Set up for biofilm growth

A membrane fouling simulator (MFS), equipped with a transparent glass window, was used to grow a biofilm [6]. The MFS contained coupons of product spacer, membrane and feed spacer, resulting in similar hydrodynamic conditions as in large scale spiral wound membrane modules. The spacer and membrane sheets were taken from virgin spiral wound membrane elements (4040-TS80-TSF, Trisep Corporation, USA). The feed spacer consisted of a sheet of 31 mil (787 μm) thick diamond-shaped polypropylene spacer (porosity 0.85). The feed spacer was placed in the MFS with the same orientation as in spiral membrane elements (45° rotation). A light–tight lid was placed on top of the glass window of the MFS to prevent growth of phototrophic organisms. The lid was removed during O_2 imaging.

The installation consisted of a pressure reducing valve, manometer, dosing point for biodegradable compounds, MFS and a flow controller (Fig. 1). The MFSs were operated at a pressure of 1.5 bar to avoid degassing and at flow rate of 16 L h^{-1} equivalent to a linear flow velocity of 0.16 m s^{-1}, which is representative for practice [18]. The MFSs were operated single pass (without partial recirculation) and without permeate production, i.e. cross flow operation only. Previous studies have shown that the presence or absence of permeate production has no effect on the measured feed channel pressure drop and biomass development during biofouling experiments [8, Supplementary material].

Water temperature was measured using a temperature sensor placed inside the tubing after the MFS. The water temperature was ~16 °C during the whole experiment.

A stock solution containing growth substrates was dosed to tap water to enhance biofilm formation. The tap water contained no residual disinfectant. A raised substrate concentration in feed water has shown to result in a faster accumulation of biomass as well as in a higher amount of accumulated biomass in membrane filter systems, leading to a faster increase in pressure drop over the MFS [18]. The solution of concentrated substrates, was dosed from a 5 L vessel into the feed water prior to the MFS by a peristaltic pump (Masterflex, Metrohm Applicon, Schiedam, The Netherlands) at a flow rate of 0.03 L h^{-1}. The dosage of substrate was checked periodically by measuring the weight of the dosing bottle. The chemicals $NaCH_3COO$, $NaNO_3$ and NaH_2PO_4 were dosed in a mass ratio C:N:P of 100:20:10. The carbon concentration in the feed water was set to 1000 μg C L^{-1}. The substrates were dissolved in ultrapure water. To restrict bacterial growth in the substrate dosage vessel, the pH was set at 11 by adding NaOH at a concentration of 1 mol L^{-1}. Stock solution vessels were replaced every 5 days. The substrate dosage flow rate (0.03 L h^{-1}) was low compared to the feed water flow rate (16 L h^{-1}). Thus, the effect of the chemical dosage on the pH of the feed water was insignificant. Biofilm grew on all surfaces inside the MFS, including the glass window. No cleaning was applied during the experiment.

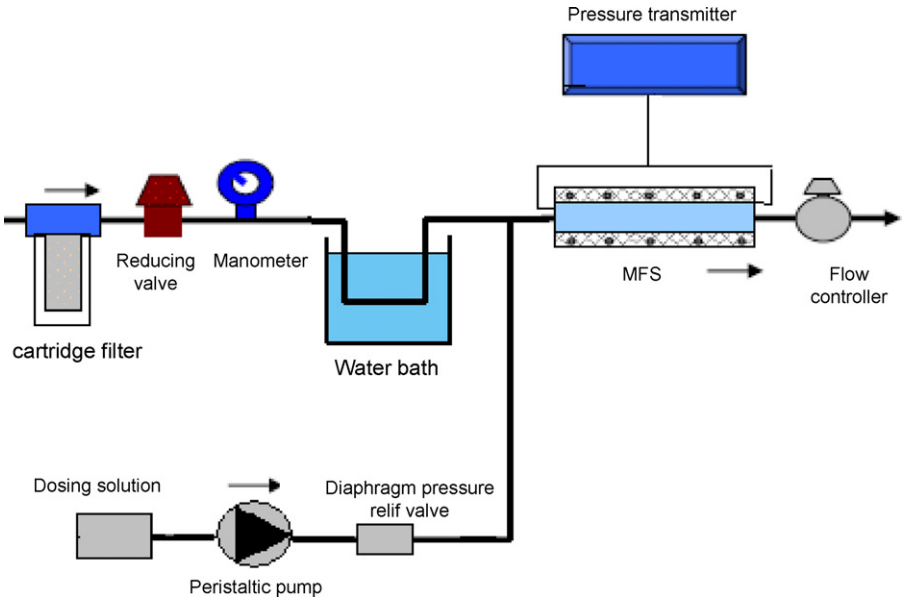

Fig. 1. Scheme of lab-scale set-up for biofouling studies. The system consisted of a cartridge filter, water bath, MFS and flow controller. The pressure drop was measured using a differential pressure transmitter. Nutrients were dosed to the MFS feed water using a peristaltic pump.

Biofilm growth was monitored by pressure drop measurements over the feed channel of the MFS, by imaging the distribution of free moving water and by imaging the O_2 distribution. Pressure drop measurements were performed using a pressure difference transmitter (type Deltabar S: PMD70-AAA7FKYAAA, Endress & Hauser, USA) with a calibration range of 0–500 mbar [19]. The imaging procedures are described below.

2.2. Set up for imaging free moving water distribution

Free flowing water was visualized by injecting 20 mL of a rhodamine WT solution (OT/US 04029NS, Chrompton & Knowles, USA) to the MFS feed water using a T-connector placed in the feed water tube before the MFS. Rhodamine WT is an inert, non-adsorbing and stable tracer for flow visualization. When the measurement was carried out immediately after injection of the solution, Rhodamine was only present in the flow channels, i.e. places were no biofilm was present. The thickness of the Rhodamine-containing water layer can be quantified by light absorbance [20]. Rhodamine WT absorbs light in the green-orange range, and light absorption is measured by the green channel of the camera. A 8 bit colour 1280 × 1024 CMOS chip camera (USB UEye SE, UI-1540-C, IDS Imaging Development Systems GmbH, Obersulm, Germany) was used to image the free flowing water distribution, as described in Staal et al. [17]. A Xenoplan XNP 1.4/17 objective (Schneider-Kreutznach, Germany) was coupled to the camera. The imaged area was illuminated using a halogen lamp (Fig. 2). The manufacturer acquisition software was used to control the image capturing procedure and to set exposure time (3.5 s) and gain per colour channel (red = 0, green = 10, blue = 30).

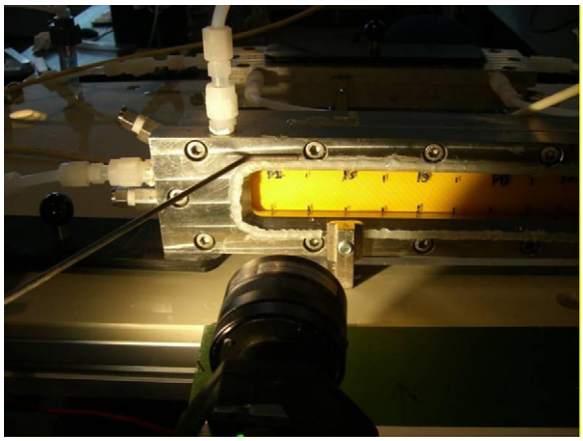

Fig. 2. Detail of experimental set-up for flow distribution imaging, showing part of the MFS glass window and camera lens. (For interpretation of the references to colour in text, the reader is referred to the web version of this article.)

2.3. Imaging of O_2 concentration

2.3.1. Measuring principle

Optodes consist of a luminescent O_2 sensitive dye, immobilized in a polymer matrix and fixed on a transparent support. The measuring principle relies on the dynamic quenching of indicator luminescence by O_2, where both luminescence intensity and luminescence lifetime vary reversibly with O_2 concentration. The quenching process does not consume O_2. Microscale optical O_2 measurements can be realized either via luminescence intensity or lifetime measurements with fibre optic microprobes [21] or by a variety of imaging configurations [16,17,22]. In this study we adapted a modular luminescence lifetime imaging system [23] to the MFS setup (Fig. 3). The oxygen sensitive dye was coated on the glass window of the MFS, so the oxygen concentration and consumption rates were only measured at the glass surface. The measuring principle behind the luminescent lifetime imaging is shown in Fig. 4. Please note that the time scale shown on this figure differed from the time of the actual measurements as described hereafter.

2.3.2. Set up for imaging O_2 concentration

The planar optode used in this study was a ruthenium-based luminescent oxygen sensitive dye (ruthenium(II)-tris-4,7-diphenyl-1,10-phenantroline; RuDpp), immobilized in a polystyrene matrix, and fixed on the sight glass of the MFS [14]. The planar optode has a thickness of ~9 μm. The RuDpp dye is suitable for O_2 imaging over a wide dynamic range, up to full saturation [16]. Imaging was performed using a monochrome 12 bit

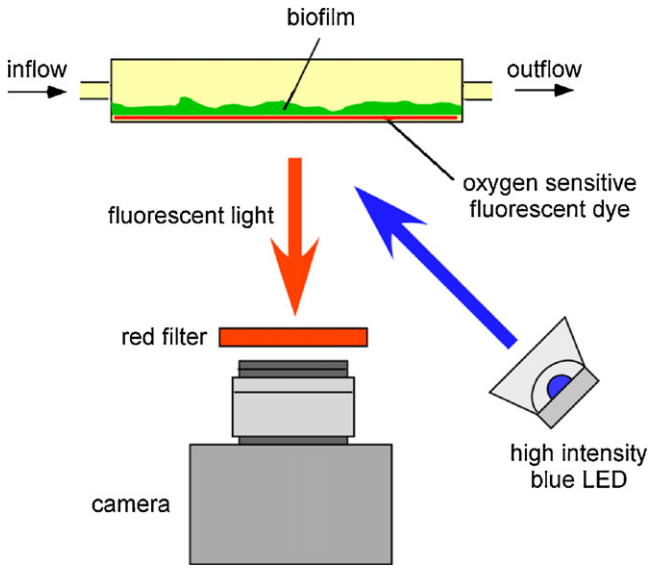

Fig. 3. Scheme of O_2 imaging set up. Oxygen measurements are performed using luminescent O_2 sensitive dyes, immobilized in a polymer matrix, fixed on a transparent support. When the dye is excited by a proper light source (typically blue LED's), both luminescent intensity and decay time are dependent on O_2 concentration. The luminescence is captured by a CCD camera equipped with a red filter to exclude background and excitation light. Timing of excitation light and camera image acquisition is done via a pulse-delay generator connected to a PC. (For interpretation of the references to colour in this figure legend, the reader is referred to the web version of the article.)

fast gate-able cooled 1280 × 1024 CCD chip camera (SENSICAM-SENSIMOD, PCO AG, Germany). The same Xenoplan objective as for water flow imaging was mounted on the camera using distance macro rings to shorten the minimum focal distance from 15 to 5–10 cm. A long-pass filter (≥590 nm, Schneider-Kreutznach, Germany) was placed on the objective to exclude background and blue excitation light. A black box was mounted around the camera set up to further exclude background light. Modulated power LED lights (1 W Luxeon Star, 470 nm, Lumileds) were used for the excitation of the dye. Excitation light was controlled by a custom built trigger delay box. The two LED's were mounted next to the objective. The capturing process was controlled using the custom made acquisition software (Look@MOLLI [15]).

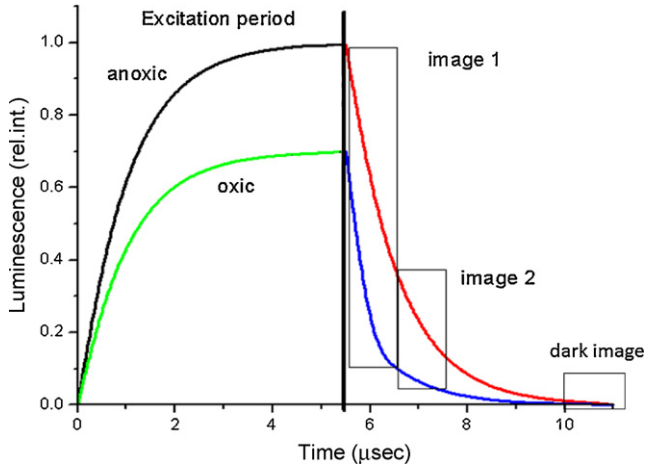

Fig. 4. Principle of luminescence lifetime measurements with O_2-sensitive optical sensors. The excitation light is turned on until the luminescence level of the dye reaches a steady state. The luminescence intensity is dependent on the O_2 concentration with maximal luminescence intensity reached under anoxic conditions. When the excitation light is switched off, the luminescence decays over time with a characteristic O_2-dependend time constant, i.e. the luminescent life time. The life time constant can be calculated from images taken in two time windows after eclipse of the excitation light. The lifetime is longest under anoxic conditions.

Luminescence intensity images were acquired sequentially by integrating series of 3 μs imaging periods obtained 0.1 μs (I_{w1}) and 4.1 μs (I_{w2}), after 4 μs excitation pulses, respectively, and followed by dark image acquisition. The total integration time per measurement period was 500 ms (see Holst et al. [23], for a detailed description of the measuring method and program). Life time (τ) images were subsequently calculated from the luminescence intensity images I_{w1} and I_{w2} images according to

$$\tau = \frac{\Delta t}{\ln(I_{W1}/I_{W2})} \quad (1)$$

where Δt is the time difference between I_{w1} and I_{w2}.

2.4. Image calculations

All post-acquisition image processing was done using the freeware *ImageJ* (http://rsbweb.nih.gov/ij/). After import to *ImageJ*, all images were converted to a 32 bit floating point format before initial thresholding. Thresholding was performed to exclude low intensity pixels, i.e. pixels within areas exhibiting no luminescence (for example areas with marker ink), from the further calculations. Lifetime images were then calculated using the "process > image calculator" option in *ImageJ*. Conversion of lifetime images to O_2 distribution images were done in the process > math > macro menu, based on calibration equation linking lifetime values to defined O_2 concentrations. False colouring was applied to visualize the differences in O_2 concentration.

2.5. Calibration

Calibration of the planar optode was done by circulating water with different O_2 concentrations through the MFS. The calibration was carried out at 16 °C, similar to the incubation temperature. Different O_2 concentrations were controlled by flushing the water with a series of defined gas mixtures controlled by an automated gas mixing system based on electronic mass flow controllers (Sensor Sense, Nijmegen). Lifetime images were taken for each defined O_2 concentration, whereby a calibration curve linking O_2 concentration and luminescence lifetime was obtained. For the calibration curve we averaged the values of a region of interest, comprising half of the imaged area, i.e. ~10 cm^2.

3. Results

3.1. Pressure drop

The time development of pressure drop over the monitor length was measured as an indicator of fouling in the MFS [18] (Fig. 5). Two phases in pressure drop development were observed: an initial phase with no or little pressure increase (days 0–4) followed by a second phase where the pressure drop showed logarithmic increase. The measurement range for the pressure drop system was 0–500 mbar, which did not allow measurements of the pressure drop accurately after day 7. The flow rate was kept constant from day 0 to day 7 but the flow could not be maintained after day 7 due to the increased resistance caused by fouling of the MFS.

The pressure drop development could be linked to biofilm growth in the MFS as observed from the colour camera pictures. Fig. 6 shows the flow distribution over the MFS length at four different time points from start of the experiment. From day 0 to day 4, free flowing water (coloured red) was observed over the total area of the MFS and no pressure drop increase was observed. From day 4, stagnant areas (yellow zones) appeared, caused by the accumulation of biomass and resulting in pressure drop increase.

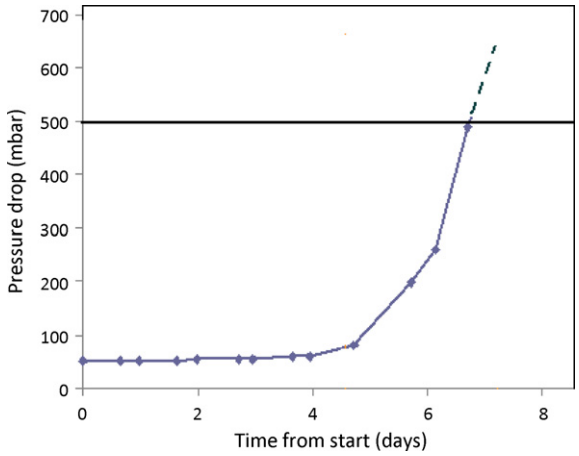

Fig. 5. Pressure drop development over time caused by fouling accumulation in MFS. The measuring limit of the differential pressure drop transmitter (500 mbar) was exceeded after 7 days.

The development of the biofilm started at the inlet of the MFS and expanded to the rest of the MFS during the following 3–4 days, leading to a logarithmically increasing pressure drop development. Channel formation was observed from day 8. Significant changes in channel structure were observed within 1 day, showing that the system was very dynamic.

3.2. Oxygen concentration

When a biofilm forms on top of the optode in the MFS it will lead to local O_2 depletion at the optode surface. The decrease in concentration will not only depend on the local activity within the biofilm but also on local biofilm thickness and the O_2 supply via the surrounding liquid-biofilm mass transfer boundary layer. When the substrate supply in the inflowing medium was switched on or off, the O_2 concentration at the optode surface reached a steady state in a few minutes (Fig. 9B). We expected to find lower O_2 concentrations in stagnant areas, corresponding to regions with thick biofilm and/or low mass transfer of O_2 towards the biofilm. Therefore, low O_2 concentrations should be indicative of the development of a biofilm. Fig. 7 shows the O_2 distribution at 4 different times during the fouling experiment. Initially, the O_2 concentration was high over the complete optode surface (red colour), which is indicative for limited fouling. With the advance of fouling, O_2 became locally depleted, in some areas even reaching anoxic conditions (blue colour). Note that the residence time of the water is very short (<2 s) and less than 10% of the O_2 in the flowing water is consumed during passage of the MFS even at the end of the experiment (data obtained with O_2 fibre sensors placed in the inlet and the outlet).

The effect of biomass accumulation on the pressure drop increase was observed earlier than the effect on oxygen concentration, suggesting that the sensitivity of the measurement needs to be improved for early detection of biofouling.

The O_2 concentration found in the flow channels on days 10 and 11 were in the range of the initial O_2 concentration at the beginning of the experiment but were higher than the O_2 concentrations found on day 9 over the optode surface. This local increase in O_2 concentration was either linked to a locally and intermittent lower amount of biomass due to detachment, or to a local higher flow rate resulting in a more efficient mass transfer of O_2. Low O_2 regions could be linked to a thick layer of biofilm or to a low mass transport phenomenon due to the absence of water flow. These stagnant regions were susceptible to show enhanced concentration polarization.

The occurrence of heterogeneous biomass distribution and development of flow channels could be clearly distinguished in the O_2 concentration images (Figs. 6 and 7). In Fig. 8 the outflow images for O_2 and biomass distribution are compared in detail, visualizing the close link between O_2 availability and presence of liquid flow. Both flow distribution and O_2 distribution images show that channelling occurred and that the flow channel distribution changed over time. Day 10 and 11 pictures show that significant differences in flow distribution occurred within 1 day, indicating that the process is dynamic.

3.3. Oxygen consumption rates

A key parameter for the study of biofilm activity is the O_2 consumption rate of the bacteria. The O_2 consumption was measured

Fig. 6. Flow distribution in time due to biofilm development. A red dye (rhodamine WT) was dosed to the MFS feed water. Red coloured areas show regions of flowing water. Yellow coloured areas show stagnant water and biomass presence. Flow direction is from left to right (arrow). The width of the flow channel is 4 cm. (For interpretation of the references to colour in this figure legend, the reader is referred to the web version of the article.)

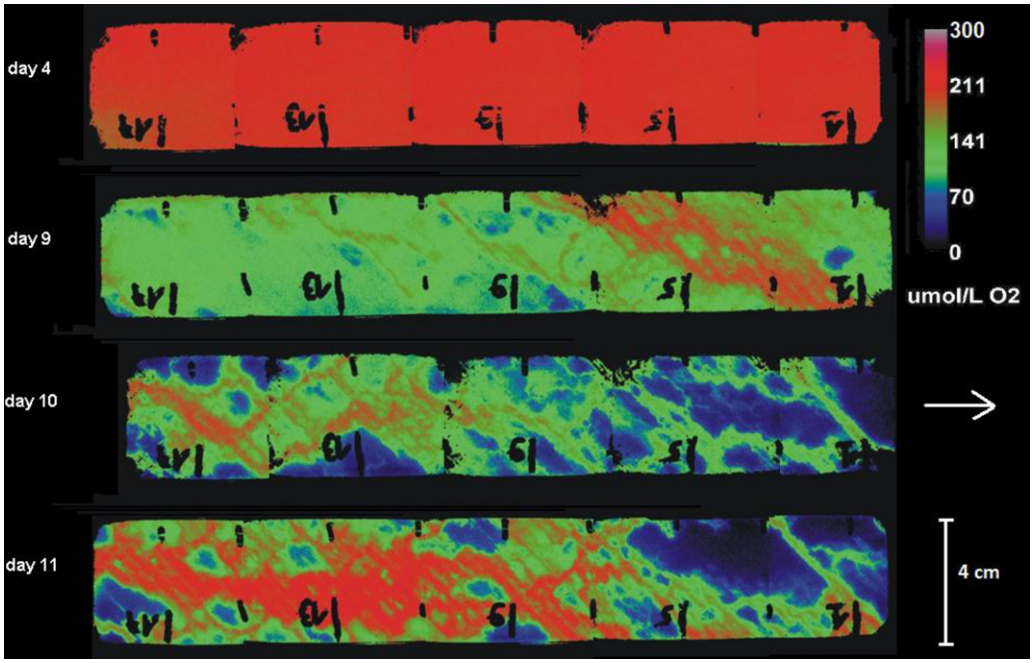

Fig. 7. Spatio-temporal distribution of O_2 concentration (μmol O_2 L^{-1}) imaged over the monitor length at the optode surface, i.e. the base of the fouling layer. The figure shows the development of low O_2 concentration regions and flow channelling over time. The flow direction is from left to right. (For interpretation of the references to colour in text, the reader is referred to the web version of this article.)

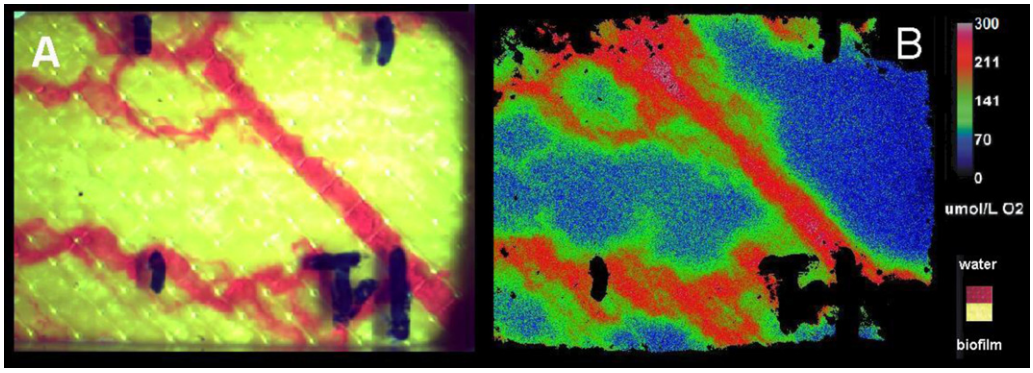

Fig. 8. Comparison of distribution of liquid flow (A) and O_2 concentration (B) on the same location at the MFS outlet side (day 10). Flow direction is from left to right. The O_2 concentration distribution is consistent with flow distribution.

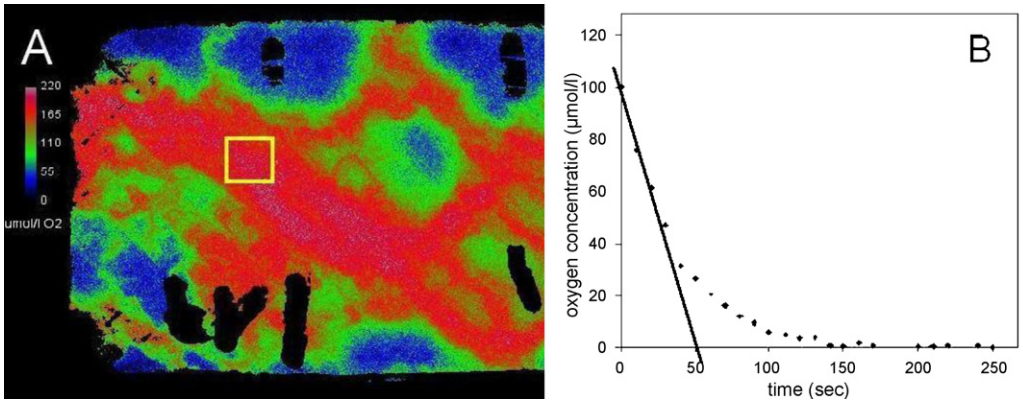

Fig. 9. Procedure to determine O_2 consumption rates in the MFS. Oxygen images were taken every 10 s after the flow was stopped. An area of interest (AOI) was selected on the initial oxygen image (A) and the O_2 depletion over time was determined for the AOI (B). The O_2 consumption rate for particular AOIs was calculated from the initial slope of the O_2 depletion curve.

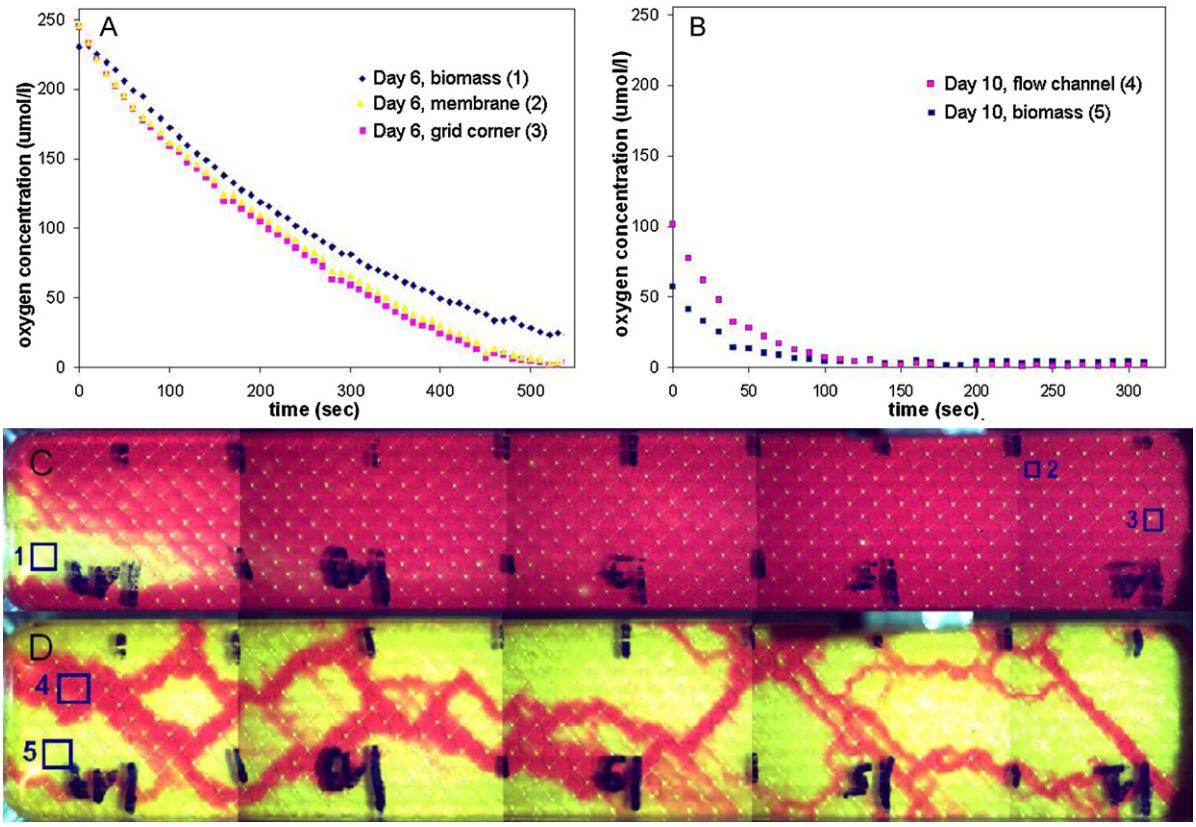

Fig. 10. Local O_2 concentration decrease over time after the water flow was stopped. Comparison of start (A) and end (B) of the experiment, for different areas in the MFS. On day 6, measurements were done (C) on a stagnant area (inlet, 1), and on two flowing regions (membrane, 2, and spacer's corner, 3). On day 10, a stagnant area and a flowing regions were compared (D). Comparison of the O_2 consumption curves on days 6 and 10 show that a steady state was reached much faster on day 10. Clear differences in slopes were found between flowing and stagnant regions.

in our system by stopping the flow and imaging the decreasing O_2 concentration at the optode surface every 10 s (Fig. 9A), from which O_2 depletion curves could be obtained for particular areas of interest (AOI) (Fig. 9B).

This procedure allows only the assessment of local activity on a thin layer at the sensor surface, but does not integrate the activity of the whole biofilm. During the first 3–5 s after the flow was stopped, the measured decrease of oxygen is mainly due to oxygen consumption of the biofilm layer directly facing the sensor [22]. However, it is important to stress that we measured over the first 10 s and therefore the observed decrease in O_2 in our system may not only reflect local O_2 consumption rates of the biofilm. Changes in O_2 transport rates could potentially affect O_2 decrease rates after the initial 5 s, due to changes in the O_2 gradient.

The O_2 concentration and O_2 consumption rate could be determined at the optode surface in time and over the MFS length (Fig. 10). With increasing MFS operating time, we observed (i) a decline in O_2 concentration (concentration at $t = 0$ in Fig. 10A and B) and (ii) an increase in O_2 consumption rates (initial slope in Fig. 10A and B). Differences in O_2 concentration and O_2 consumption rates on two locations over the monitor width (location in Fig. 10D, codes 4 and 5 and O_2 data in Fig. 10B) could be linked to the presence of stagnant and free flowing areas. This suggests that flow channelling occurred, supporting the visual observations with the dye (Fig. 10D).

A clear relationship between local O_2 consumption rates and O_2 concentration was found during analysis of the MFS outlet side O_2 data from day 10 (Fig. 11). The O_2 consumption rates were highest for the high O_2 concentrations (Fig. 11). It is usually assumed that active biomass is non-homogeneously distributed with depth within biofilms. Upper parts of biofilms are directly supplied with

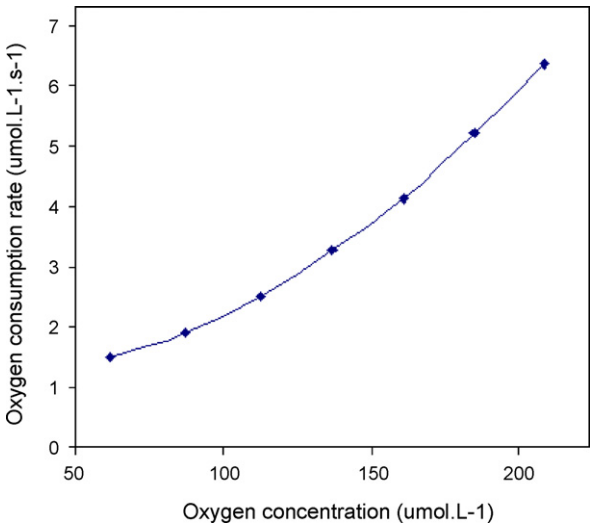

Fig. 11. Relationship between O_2 consumption and O_2 concentration. This curve was obtained by analyzing the oxygen image of the MFS outlet side, day 10. Pixels with a value included in a defined O_2 concentration range were selected and the O_2 decrease of the corresponding pixels was calculated and averaged. This procedure was performed for 7 different O_2 concentration ranges with a width of 25 μmol L^{-1}.

O_2 and substrate, while deeper parts can be mass transfer or substrate limited in O_2 and/or organic substrate. Therefore higher growth rates and metabolic activity can be expected in upper layers of thick biofilms. In our experiment oxygen concentrations and consumption rates were assessed on the deepest layer of the biofilm, directly at the optode surface. Areas covered with a very

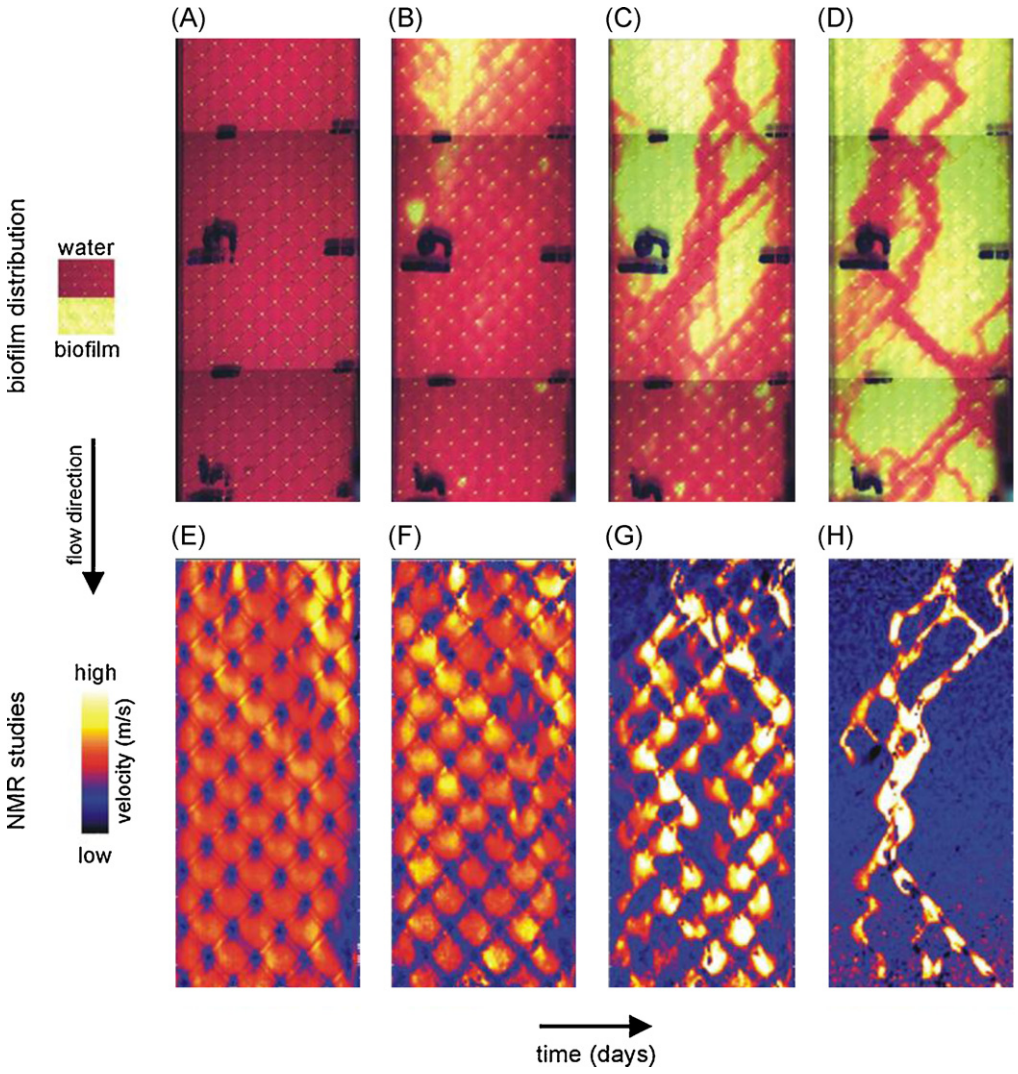

Fig. 12. Flow channel development in the MFS monitored by the addition of Rhodamine WT dye (A–D) and liquid velocity field distribution (E–H) measured in the MFS with NMR.
Adapted from Schulenberg et al. [7].

thin biofilm would have high activities as well as high O_2 concentrations close to the optode surface, while lower activities and low O_2 concentrations would be measured in stagnant zones in the deepest layer of a thick biofilm.

4. Discussion

Our study demonstrated that spatially resolved O_2 concentrations and O_2 consumption rates can be quantified during biofilm accumulation in a membrane fouling simulator (MFS) equipped with a planar optode (Figs. 7 and 10). It was shown that the O_2 concentration can be used as an indicator of biofilm presence in the MFS, since a good correlation was found between O_2 concentration and liquid flow distributions (Figs. 6–8). The O_2 consumption rate measurements were sensitive enough to distinguish high and low biological activity areas and thus can be used as method to detect and quantify biological activity in the MFS.

4.1. Structural information: flow channels observation

Our measurements showed the development of flow channels in the biofilms (Figs. 6 and 7), which is consistent with the results of studies applying other methods such as autopsy of membrane modules from full scale NF and RO installations [9] and NMR studies on flow cells (Fig. 12). With NMR, flow velocity fields were measured over time in a flow cell, showing changes in flow velocity fields due to biofilm development and formation of flow channels in the biofilms [7,8]. Three-dimensional numerical models [9], developed to determine hydrodynamics and biofouling in the feed spacer channels [10] showed flow channel formation as well. The flow channelling indicates that the total membrane system is very dynamic, since the flow distribution profile can change completely within a short time (Fig. 7). The visualized stagnant regions may explain enhanced concentration polarization and reduced membrane performance observed in real membrane systems. Optodes could therefore help in studying declining membrane performance (increased feed channel pressure drop and salt passage and decreased flux) caused by biofouling.

4.2. A new tool for activity information: strengths and limitations

A previous study on biofouling activity quantification addressed assessment of O_2 consumption rates in membrane installations by measuring the O_2 concentration of the water before and after passing the installation (feed and concentrate), but such measurements were not suitable to assess the biofouling activity during

membrane operation [24]. Attempts to establish a mass balance for biological processes in membrane systems by analysing the feed, the concentrate and the permeate waters have not resulted in a closed mass balance (using parameters like ATP, TDC, BDOC, AOC and BFR; unpublished data). Thus, no suitable method has hitherto been identified for non-destructive assessment of biological activity in membrane systems.

The present study showed that optode-based measurements of O_2 consumption rates were sensitive enough to distinguish regions with large differences in O_2 consumption activity and therefore could be used as a biological activity indicator. However, careful interpretation of the results is needed since the O_2 concentrations and consumption rates are only measured at the surface of the optode, representative only for a thin layer of biofilm. Such measurements showed only the processes occurring on the membrane surface and are not representative for the whole biofilm grown on the optode surface. In principle, the O_2 sensitive dye can also be coated on the feed spacer for additional data on the biofouling process but such an approach needs further optimization (data not shown).

The presented method has clear advantages. The equipment needed for optode studies is relatively small, easy to transport and to handle. Even simpler systems based on ratiometric O_2 imaging [17] can be implemented. A standardized user friendly imaging unit with a fixed position of LEDs relative to the camera position and automatic data processing software is under development, simplifying the imaging and data processing for regular measurements or long term laboratory studies, and improving the sensitivity of the measurements.

A current disadvantage is that the distribution of extracellular polymeric substances (EPS) in the MFS are not measured. EPS is considered as an important factor in biofouling of membrane systems [25] and its effect cannot be studied by this method.

4.3. Applications

Non-destructive biofouling diagnosis is important for early biofouling detection and effective control strategies in membrane filtration systems. The MFS was shown to be a suitable tool for early warning of fouling [6,26] when used in combination with sensitive pressure drop measurements. Pressure drop measurements are indicative for fouling but do not indicate which type of fouling occurs. Combining these measurements with activity measurements using optodes would allow more precise diagnosis of biofouling. The optode can only be used in a monitor (either with or without permeate production) installed in parallel to the membrane filtration installation. However, further improvements e.g. of the illumination system, camera settings or O_2 indicator chemistry (adapted for a low range of O_2 concentrations) are needed for early detection of biofilm formation.

The O_2 sensitive dye is stable under saline conditions (seawater) and has been used already for studies in marine sediments [15,27]. Thus, similar optode imaging setups could also be applied for diagnosis or early warning of biofouling in desalination plants.

From a research point of view, flow profiles and biomass distribution were already provided by NMR and hydrodynamic parameters by modelling. However, the activity parameter was lacking. Earlier attempts to quantify activity involved measurements of Adenosine Tri-Phosphate (ATP) [5], involving destructive membrane autopsy. Non destructive activity measurements using O_2 consumption rates are a step forward for laboratory and on-site monitoring biofouling studies in membrane systems, allowing non-invasive activity measurement over time to gain insight in the biofouling process and evaluate the effect of biofouling control actions. The combination of activity measurements using optodes, flow profiles and biomass distribution using NMR, and hydrodynamic parameters using modelling could provide a comprehensive and full overview of biofouling processes.

5. Conclusions

By adapting planar O_2 optodes and a luminescence imaging system to a membrane fouling simulator we were for the first time able to perform direct biological activity measurements of biofouling in operating membrane systems. This new approach has a large potential for application in membrane systems and has the following advantages:

1. O_2 measurements using optodes can provide both structural information and quantitative activity measurements of biofouling.
2. The method is non-destructive, the equipment is small and easy to handle and can be easily combined with sensitive pressure drop measurements.
3. The method enables non-destructive biofouling diagnosis. With further improvement it could be a useful tool for early detection of biofouling.
4. The presented quantitative biological activity method is complementary with other methods to study biofouling control such as MRI, MFS and numerical modelling.

Acknowledgements

This work was performed by Wetsus, centre of excellence for sustainable water technology, Delft University of Technology and the Marine Biological Laboratory, University of Copenhagen. Wetsus is funded by the Ministry of Economic Affairs. Additional support was due to grants from the Danish Natural Science Research Council (M.S., M.K.). The authors thank the participants of the Wetsus theme 'Biofouling' for the fruitful discussions and their financial support.

Appendix A. Supplementary data

Supplementary data associated with this article can be found, in the online version, at doi:10.1016/j.memsci.2011.12.003.

References

[1] W.G. Charaklis, K.C. Marshall, Biofilms, John Wiley & Sons, New York, 1990.
[2] H.C. Flemming, G. Schaule, T. Griebe, T. Schmitt, A. Tamachkiarowa, Biofouling—the Achilles heel of membrane processes, Desalination 113 (2-3) (1997) 215–225.
[3] D.H. Paul, Reverse osmosis: scaling, fouling & chemical attack, Desalination Water Reuse 1 (1991) 8–11.
[4] D.H. Paul, Membranes: biofouling of reverse osmosis units, Ultrapure Water (1996) 64–67.
[5] J.S. Vrouwenvelder, S.A. Manolarakis, J.P. Van der Hoek, J.A.M. Van Paassen, W.G.J. Van der Meer, J.M.C. Van Agtmaal, H.D.M. Prummel, J.C. Kruithof, M.C.M. Van Loosdrecht, Quantitative biofouling diagnosis in full scale nanofiltration and reverse osmosis installations, Water Res. 42 (2008) 4856–4868.
[6] J.S. Vrouwenvelder, J.A.M. Van Paassen, L.P. Wessels, A.F. Van Dam, S.M. Bakker, The membrane fouling simulator: a practical tool for fouling prediction and control, J. Membr. Sci. 281 (2006) 316–324.
[7] D.A. Graf von der Schulenberg, J.S. Vrouwenvelder, S.A. Creber, M.C.M. Van Loosdrecht, M.L. Johns, Nuclear magnetic resonance microscopy studies of membrane biofouling, J. Membr. Sci 323 (2008) 37–44.
[8] J.S. Vrouwenvelder, D.A. Graf von der Schulenberg, J.C. Kruithof, M.L. Johns, M.C.M. van Loosdrecht, Biofouling of spiral wound nanofiltration and reverse osmosis membranes: a feed spacer problem, Water Res. 43 (2009) 583–594.
[9] J.S. Vrouwenvelder, C. Picioreanu, J.C. Kruithof, M.C.M. Van Loosdrecht, Biofouling in spiral wound membrane systems: three-dimensional CFD model based evaluation of experimental data, J. Membr. Sci. 346 (2010) 71–85.
[10] C. Picioreanu, J.S. Vrouwenvelder, M.C.M. Van Loosdrecht, Three-dimensional numerical modeling of biofouling and fluid dynamics in feed spacer channels of membrane devices, J. Membr. Sci. 345 (2009) 340–354.
[11] T. Fenchel, B. Finlay, Oxygen and the spatial structure of microbial communities, Biol. Rev. 83 (2008) 553–569.

[12] R.N. Glud, N.B. Ramsing, J.K. Gundersen, I. Klimant, Planar optodes: a new tool for fine scale measurements of two-dimensional O_2 distribution in benthic communitie, Mar. Ecol. Prog. Ser. 140 (1996) 217–226.
[13] R.N. Glud, C.M. Santegoeds, D. De Beer, O. Kohls, N.B. Ramsing, Oxygen dynamics at the base of a biofilm studied with planar optodes, Aquat. Microb. Ecol. 14 (1998) 223–233.
[14] M. Kühl, L.F. Rickelt, R. Thar, Combined imaging of bacteria and oxygen in biofilms, Appl. Environ. Microbiol. 73 (19) (2007) 6289–6295.
[15] G. Holst, B. Grunwald, Luminescence lifetime imaging with transparent oxygen optodes, Sens. Actuators B 74 (2001) 78–90.
[16] M. Kühl, L. Polerecky, Functional and structural imaging of phototrophic microbial communities and symbioses, Aquat. Microb. Ecol. 53 (2008) 99–118.
[17] M. Staal, E.I. Prest, J.S. Vrouwenvelder, L.F. Rickelt, M. Kühl, A simple optode based method for imaging O_2 distribution and dynamics in tap water biofilms, Water Res. 45 (2011) 5027–5037.
[18] J.S. Vrouwenvelder, C. Hinrichs, W.G.J. Van der Meer, M.C.M. Van Loosdrecht, J.C. Kruithof, Pressure drop increase by biofilm accumulation in spiral wound RO and NF membrane systems: role of substrate concentration, flow velocity, substrate load and flow direction, Biofouling 25 (2009) 543–555.
[19] J.S. Vrouwenvelder, J.A.M. Van Paassen, J.C. Kruithof, M.C.M. Van Loosdrecht, Sensitive pressure drop measurements of individual lead membrane elements for accurate early biofouling detection, J. Membr. Sci. 338 (2009) 92–99.
[20] M. Huettel, W. Ziebis, S. Forster, Flow-induced uptake of particulate matter in permeable sediments, Limnol. Oceanogr. 41 (1996) 309–322.
[21] M. Kühl, Optical microsensors for analysis of microbial communities, Methods Enzymol. 397 (2005) 166–199.
[22] M. Staal, S. Borisov, L.F. Rickelt, I. Klimant, M. Kühl, Ultrabright planar optodes for luminescence life-time based microscopic imaging of O_2 dynamics in biofilms, J. Microbiol. Methods 85 (2011) 67–74.
[23] G. Holst, O. Kohls, I. Klimant, B. König, M. Kühl, T. Richter, A modular luminescence lifetime imaging system for mapping oxygen distribution in biological samples, Sens. Actuators B 51 (1998) 163–170.
[24] J.W.N.M. Kappelhof, H.S. Vrouwenvelder, M. Schaap, J.C. Kruithof, D. Van Der Kooij, J.C. Schippers, An in situ biofouling monitor for membrane systems, Water Sci. Technol. Water Supply 3 (5–6) (2003) 205–210.
[25] IWA. International Biofouling Workshop, Singapore, Nanyang Technological University (July 2011) pp. 1–3.
[26] J.S. Vrouwenvelder, M.C.M. Van Loosdrecht, J.C. Kruithof, Early warning of biofouling in spiral wound nanofiltration and reverse osmosis membranes, Desalination 265 (2011) 206–212.
[27] R.N. Glud, A. Tengberg, M. Kühl, P.O.J. Hall, I. Klimant, G. Holst, An *in situ* instrument for planar O_2 optode measurements at benthic interfaces, Limnol. Oceanogr. 46 (2001) 2073–2080.
[28] L.Y. Dudley, E.G. Darton, Membrane autopsy – a case study, Desalination 105 (1996) 135–141.
[29] S.A. Creber, T.R.R. Pintelon, D.A.W. Graf von der Schulenburg, J.S. Vrouwenvelder, M.C.M. van Loosdrecht, M.L. Johns, Magnetic resonance imaging and 3D simulation studies of biofilm accumulation and cleaning on reverse osmosis membranes, Food Bioprod. Process. 88 (2010) 401–408.
[30] A.I. Radu, J.S. Vrouwenvelder, M.C.M. van Loosdrecht, C. Picioreanu, Modeling the effect of biofilm formation on reverse osmosis performance: flux, feed channel pressure drop and solute passage, J. Membr. Sci. 365 (2010) 1–15.